Silver clusters insert into polymer solar cell for enhancing light absorption

Guolong Li (李国龙), Hongyu Zhen (甄红宇)*, Zhuoyin Huang (黄卓寅), Kan Li (李 衍), Weidong Shen (沈伟东), and Xu Liu (刘 旭)

State Key Laboratory of Modern Optical Instrumentation, Zhejiang University, Hangzhou 310027, China

**Corresponding author: hongyuzhen@zju.edu.cn*

Received March 28, 2011; accepted May 28, 2011; posted online August 24, 2011

As an employment of surface plasmonic effect, the consequence of insertion of a layer of Ag clusters into polymer solar cell on the enhancement of light absorption and power conversion efficiency is investigated. Optical analysis based on the finite-difference time-domain (FDTD) is performed with experiments to evaluate the effect of the interaction between the Ag clusters and incident light on light absorption in polymer solar cell. Ag clusters modify the light wave vector and the electromagnetic field inside the device is redistributed and enhanced. As a result, polymer solar cells achieve an overall increase in absorption, short-circuit current density, and power conversion efficiency.

OCIS codes: 240.6680, 350.6050, 290.5850.
doi: 10.3788/COL201210.012401.

Low conversion efficiency of the polymer solar cell is attributed to the weak absorption of the thin active layer owing to the existing trade-off between optical absorption and electrical performance[1−3]. Structuring the thin-film solar cell for light-trapping has resulted in enhancement of optical absorption under a special spectral range without increasing the active layer thickness[4−10]. Another promising device architecture can be accomplished with Ag clusters embedded into the device. This can enhance electromagnetic field intensity (EFI) near the active layer due to Ag plasmonic effects[11−16]. Plasmonic polymer solar cell has been intensively studied with the aim of promoting cell conversion efficiency[17−19]. However, only a few studies have reported on the redistribution and the enhancement of EFI inside the polymer solar cell due to the insertion of Ag clusters.

In this letter, the insertion of a thin layer of Ag clusters into the polymer solar cell facilitated increased optical absorption in the active layer over a broad range of visible wavelengths. The finite-difference time-domain (FDTD) method was applied to analyze the distribution of electromagnetic intensity inside the polymer solar cell with the Ag clusters and determine the effect of the interaction between the clusters and incident light on the intensity enhancement of the polymer solar cell[20−22].

The layer of Ag clusters was deposited by thermally evaporating Ag powder (99.95%, Aladdin) onto a cleaned indium tin oxide (ITO) substrate at 10^{-6} and subsequently annealed at 250 °C in a glove box with nitrogen. The thickness of the layer was monitored *in-situ* by a quartz crystal oscillator. The reference device was treated with oxygen. No plasma treatment was performed on the device with Ag clusters. The polymer solar cell was fabricated with the structure of ITO (∼150 nm) /Ag cluster layer / PEDOT:PSS (∼40 nm) / P3HT:PCBM (∼100 nm) /LiF (1 nm) /Al (120 nm)[23], as presented in Fig. 1.

For convenience of description, the device without Ag clusters serves as the reference device and the device with 7.8-nm-thick Ag clusters is the device that is investigated. The current density-voltage ($J-V$) measurements of the device were performed with a semiconductor characterization system (4155C Agilent, USA) under the excitation of a 450-W solar simulator (oriel 94023, Newport, USA) using an AM 1.5 filter at the intensity of 80 mW/cm^2. Incident photon conversion efficiency (IPCE) was recorded using an IPCE measurement system (Shanghai Koan Electro-Optics Co., Ltd), as presented in Fig. 2.

In Fig. 2, IPCE increases at the light wavelength from 350 to 630 nm. Short circuit current density J_{sc} increases from 8.5 to 10.2 mA/cm^2. Power conversion

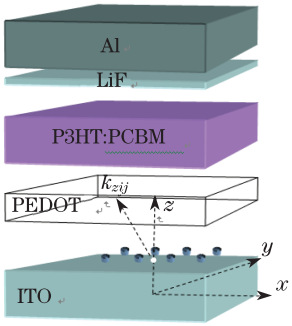

Fig. 1. Structure of the device with the layer of Ag clusters.

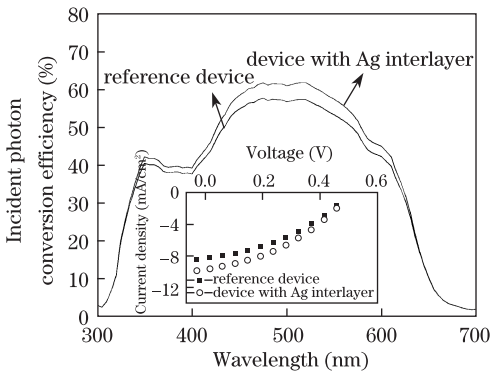

Fig. 2. Incident photon conversion efficiency and $J-V$ (inset) for the devices with and without Ag clusters.

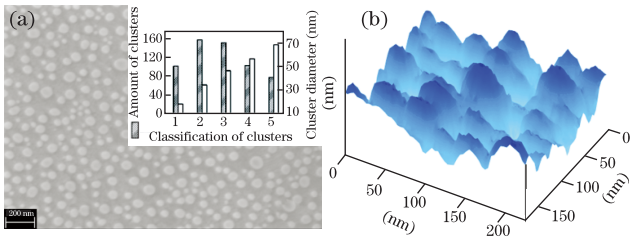

Fig. 3. (a) SEM and (b) AFM images of the Ag clusters on ITO substrate.

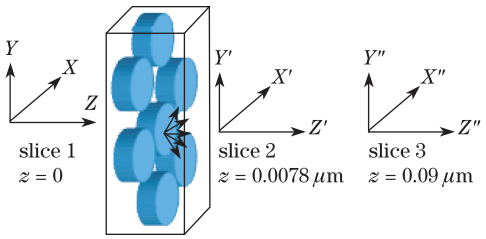

Fig. 4. Equivalent physical model of Ag cluster.

efficiency (PCE) for the device with Ag clusters η_{Ag} is 1.79%, a factor of 27% increases with respect to the reference device η_{ref} of 1.40%. The fill factor (FF) decreases from 40.49% to 39.75%, which indicates no apparent change. Thus, the increase of conversion efficiency results from the increased short-circuit current because of the existence of Ag clusters. With the integration of the incident photon coversion efficiency (IPCE) over 300–700-nm wavelength, J_{sc} is 7.79 mA/cm^2 for the reference device and 8.29 mA/cm^2 for the Ag cluster device. Compared with $J-V$ curves, lower J_{sc} from IPCE is caused by the mismatch of spectra of two light source and the performance degradation of unencapsulated device.

Scanning electron microscopy (SEM) (SmartSEM V5.00 Carl Zeiss, German) and atomic force microscopy (AFM) (SPI3800N, Seiko, Japan) images of Ag clusters were obtained. These are shown in Fig. 3. The size of the clusters was analyzed by the software Image-Pro Plus version 6.0.0.260. Based on the images, a unit cell was physically modeled and shown in Fig. 4. Six discs with a diameter of $d = 40$ nm are positioned at the corners of a hexagon and another disc with the same diameter is centered in the hexagon. The distance between two discs is 50 nm. PEDOT:PSS is surrounding the discs.

Particle polarizability α is given as

$$\alpha = 3V\frac{\varepsilon - \varepsilon_{\mathrm{m}}}{\varepsilon + 2\varepsilon_{\mathrm{m}}}, \tag{1}$$

where V is the particle volume and ε and ε_{m} are the particle and surrounding medium dielectric functions, respectively. When $\varepsilon_{\mathrm{Ag}} = -2\varepsilon_{\mathrm{PEDOT}}$, the particle polarizability will become very large and the incident light will be strongly scattered at the wavelength near the plasmon resonance.

FDTD method was applied to evaluate the influence of the plasmonic resonance effect on the electromagnetic field distribution inside the device shown in Fig. 4[21]. Mesh size of 0.4–1 nm in the vicinity of the metal cluster was used in the simulation. EFI versus wavelength at the slice 2: $z = 0.0078$ μm is shown in Fig. 5.

Figure 5 shows that the electromagnetic intensity is magnified more over a broad range of visible wavelengths at the slice 2 inside the device with Ag clusters compared with the reference. The peak wavelength of the electromagnetic intensity red-shifts from 485 to 575 nm and the electromagnetic intensity is enhanced by a factor of 35.3. The light is scattered by the clusters and the scattering field is formed. The scattering field amplifies the EFI in the polymer solar cell and the intensity of field as a function of the incident light wavelength is maximized at 575 nm in the vicinity of Ag clusters.

For the reference device, the normalized EFI values of slice 2 are 0.884 and 0.337 at light wavelengths of 500 and 575 nm, respectively. For slice 3, the values are 0.669 and 1.163 at light wavelengths of 500 and 575 nm, respectively. The Ag cluster device presents nonidentical EFI at slice 2 and slice 3, as presented in Fig. 6. In Figs. 6(a) and (b), the maximum value of EFI is larger than 90 in slice 2 of Ag cluster device when the excitation wavelength is 575 nm. Several maxima appear among the Ag clusters. In Figs. 6(c) and (d), the enhanced EFI is observed in the device which is not the case with the reference. Thus, EFI near the active layer is

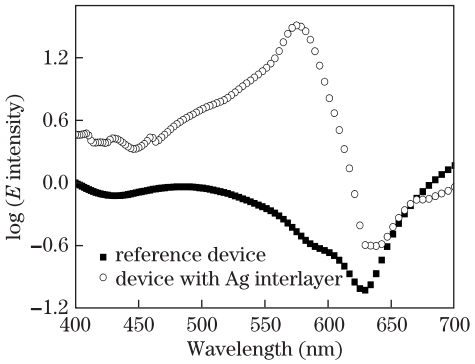

Fig. 5. Electromagnetic intensity versus wavelength for the point of $x = 0$, $y = 0$, $z = 0.0078$ μm in the devices.

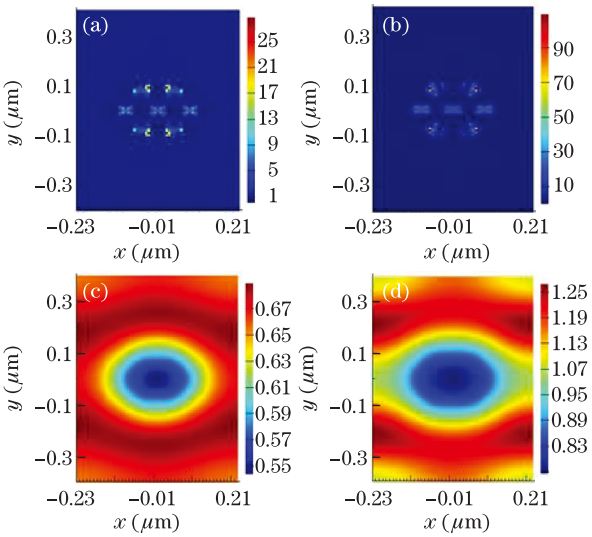

Fig. 6. Electromagnetic intensity versus position (x,y) at: (a) 500-nm and (b) 575-nm wavelengths for the slice 2: $z = 0.0078$ μm in the device with Ag clusters, (c) 500-nm and (d) 575-nm wavelengths for the slice 3: $z = 0.09$ μm in the device with Ag clusters.

apparently redistributed and enhanced for the existence of Ag clusters. This confirms that the near-field radiative coupling between the incident light and the small clusters modifies the incident lightwave vector. The sunlight scattered with large angle enhances the electromagnetic field in the active layer leading to the increased absorption.

In conclusion, polymer solar cell with a layer of Ag clusters shows an overall increase in absorption, short-circuit current density, and power conversion efficiency compared with the reference device. Based on the SEM and AFM images, light absorption enhancement is attributed to the redistribution and enhancement of EFI caused by the Ag clusters as confirmed by FDTD simulation.

This work was supported by the National Natural Science Foundation of China (No. 61007056), the Research Fund for the Doctoral Program of Higher Education of China (No. 20100101120048), the Fundamental Research Funds for the Central Universities (Nos. 2009QNA5010 and 2010QNA6003), and the Educational Office of Zhejiang Province (No. Y200803562).

References

1. J. Y. Kim, K. Lee, N. E. Coates, D. Moses, T. Q. Nguyen, M. Dante, and A. J. Heeger, Science **317,** 222 (2007).
2. C. Cocoyer, L. Rocha, L. Sicot, B. Geffroy, R. de Bettignies, C. Sentein, C. Fiorini-Debuisschert, and P. Raimond, Appl. Phys. Lett. **88,** 133108 (2006).
3. S. B. Rim, S. Zhao, S. R. Scully, and M. D. McGehee, and P. Peumans, Appl. Phys. Lett. **91,** 243501 (2007).
4. R. Bouffaron, L. Escoubas, J. J. Simon, Ph. Torchio, F. Flory, G. Berginc, and Ph. Masclet, Opt. Express **16,** 19304 (2008)
5. C. Ulbrich, M. Peters, B. Bläsi, T. Kirchartz, A. Gerber, and U. Rau, Opt. Express **18,** A133 (2010).
6. S. I. Na, S. S. Kim, J. Jo, S. H. Oh, J. Kim, and D. Y. Kim, Adv. Funct. Mater. **18,** 3956 (2008).
7. L. S. Roman, O. Inganäs, T. Granlund, T. Nyberg, M. Svensson, M. R. Andersson, and J. C. Hummelen, Adv. Mater. **12,** 189 (2000).
8. K. Nakayama, K. Tanabe, and H. A. Atwater, Appl. Phys. Lett. **93,** 121904 (2008).
9. H. A. Atwater and A. Polman, Nat. Mater. **9,** 205 (2010).
10. Y. M. Bai, H. Zhang, J. Wang, N. F. Chen, J. X. Yao, T. M. Huang, X. W. Zhang, Z. G. Yin, and Z. Fu, Chin. Opt. Lett. **9,** 032901 (2011).
11. G. Xu, M. Tazawa, P. Jin, S. Nakao, and K. Yoshimura, Appl. Phys. Lett. **82,** 3811 (2003).
12. Z. Kam, Nature **306,** 625 (1983).
13. K. R. Catchpolea and A. Polmanb, Appl. Phys. Lett. **93,** 191113 (2008).
14. S. Pillai, K. R. Catchpole, T. Trupke, and M. A. Green, J. Appl. Phys. **101,** 093105 (2007).
15. K. Tvingstedt, N. K. Persson, and O. Inganäs, Appl. Phys. Lett. **91,** 113514 (2007).
16. S. S. Kim, S. I. Na, J. Jo, D. Y. Kim, and Y. C. Nah, Appl. Phys. Lett. **93,** 073307 (2008).
17. W. J. Yoon, K. Y. Jung, J. Liu, T. Duraisamy, R. Revur, F. L. Teixeira, S. Sengupta, and P. R. Berger, Solar Energy Mater. Solar Cells **94,** 128 (2010).
18. K. R. Catchpole and A. Polman, Opt. Express **16,** 21793 (2008).
19. P. Royer, J. P. Goudonnet, R. J. Warmack, and T. L. Ferrell, Phys. Rev. B **35,** 3753 (1987).
20. Y. D. Yang, S. J. Wang, and Y. Z. Huang, Chin. Opt. Lett. **8,** 502 (2010).
21. D. B. Sullivan, *Electromagnetic Simulation Using the FDTD Method* (IEEE Press, New York, 2000).
22. F. Monestiera, J. J. Simona, P. Torchioa, L. Escoubasa, F. Florya, S. Baillyb, R. Bettigniesb, S. Guillerezb, and C. Defranouxc, Solar Energy Mater. Solar Cells **91,** 405 (2007).
23. G. Li, V. Shrotriya, J. Huang, Y. Yao, T. Moriarty, K, Emery, and Y. Yang, Nature Materials **4,** 864 (2005).